Dissolved organic matter biodegradation along a hydrological continuum in permafrost peatlands

Daheydrey Payandi-Rolland, Liudmila Shirokova, Marwa Tesfa, Pascale Benezeth, Artyom Lim, Daria Kuzmina, Jan Karlsson, Reiner Giesler, Oleg S Pokrovsky

Dissolved organic matter biodegradation along a hydrological continuum in permafrost peatlands

D. Payandi-Rolland[1*], L.S. Shirokova[1,2], M. Tesfa[1], P. Bénézeth[1], A.G. Lim[3], D. Kuzmina[3], J. Karlsson[4], R. Giesler[4], O.S. Pokrovsky[1,2,3]

[1] *Geoscience and Environment Toulouse, GET-CNRS-IRD-OMP, University of Toulouse, 14, Avenue Edouard Belin, 31400 Toulouse, France*

[2] *Institute of Ecological Problems of the North, N. Laverov Federal Center for Integrated Arctic Research, Arkhangelsk, Russia*

[3] *BIO-GEO-CLIM Laboratory, Tomsk State University, 35 Lenina Pr., Tomsk, Russia*

[4] *Climate Impacts Research Centre (CIRC), Department of Ecology and Environmental Science, Umeå University, SE-981 07 Abisko, Sweden*

*corresponding author email: dahedrey.payandi-rolland@get.omp.eu

Keywords: river, stream, thermokarst lake, supra-permafrost water, carbon dioxide emission, low molecular weight organic acids

Key sentences:

- We compared surface waters of two hydrological continuums (HC) in northern Sweden and western Siberia
- Large spatial heterogeneity of dissolved organic carbon concentration and biodegradability along HC.
- Along the HC from supra-permafrost waters, fens, and ponds to lakes, streams and rivers, the DOC removal rate decreased and the BDOC increased.

- BDOC ranged from 0 to 20% and could at the most account for 10% of CO_2 emissions from surface waters of these permafrost peatlands

Abstract

Arctic regions contain large amounts of organic carbon (OC) trapped in soil and wetland permafrost. With climate warming, part of this OC is released to aquatic systems and degraded by microorganisms, thus resulting in positive feedback due to carbon (C) emission. In wetland areas, water bodies are spatially heterogenic and separated by landscape position and water residence time. This represents a hydrological continuum, from depressions, smaller water bodies and lakes to the receiving streams and rivers. Yet, the effect of this heterogeneity on the OC release from the soil and its processing in waters is largely unknown and not accounted for in C cycle models of Arctic regions. Here we investigated the dissolved OC (DOC) biodegradation of aquatic systems along a hydrological continuum located in two discontinuous permafrost sites: in western Siberia and northern Sweden. The biodegradable dissolved OC ($BDOC_{15}$; % DOC lost relative to the initial DOC concentration after 15 days incubation at 20°C) ranged from 0 to 20% for small water bodies located at the beginning of the continuum (soil solutions, small ponds, fen and lakes) and from 10 to 20% for streams and rivers. While the $BDOC_{15}$ increased, the removal rate of DOC decreased along the hydrological continuum. The potential maximum CO_2 production from DOC biodegradation was estimated to account for only a small part of *in-situ* CO_2 emissions measured in peatland aquatic systems of northern Sweden and western Siberia. This suggests that other sources, such as sediment respiration and soil input, largely contribute to CO_2 emissions from small surface waters of permafrost peatlands. Our results highlight the need to account for large heterogeneity of dissolved OC concentration and biodegradability in order to quantify C cycling in arctic water bodies susceptible to permafrost thaw.

1. Introduction

The carbon (C) released from thawing permafrost is biotically and abiotically processed in aquatic systems (Abbott et al., 2016; Cory and Kling, 2018; Mann et al., 2015). However, the degree and intensity of this processing are strongly variable both in space (local to global scale) and time (day/night to season) and not explicitly accounted for in global modelling of permafrost-carbon-climate feedback. The spatial variability includes the various types of water bodies of those regions, all belonging to the hydrological continuum (Figure 1). Globally, the concept of 'hydrological continuum' (Creed et al., 2015; Palmer et al., 2016) includes the movement of water from sources (soil and supra-permafrost waters) to intermediate reservoirs (lakes and streams) and finally into terminal reservoirs (large rivers and their estuaries). In Arctic regions, the hydrological continuum (HC) is highly dependent on the maturation cycle of water bodies. All steps of HC are especially important as they can influence the biochemical properties, photo- (Panneer Selvam et al., 2019) and bio-degradability (Liu et al., 2019; Vonk et al., 2015) of dissolved organic matter (DOM). Since the transport of thawed permafrost organic C can spatially relocate the emissions of greenhouses gases (Vonk and Gustafsson, 2013), the heterogeneity of waterbodies observed along a hydrological continuum is a key point to understand the C cycle in these regions.

Dissolved organic carbon (DOC) is the main form of terrestrial organic carbon (OC) exported to soil solution, rivers, wetlands and lakes (Chapin et al., 2006; Cole et al., 2007). This is especially true in the case of discontinuous permafrost regions, where the hydrologic flow paths have longer residence times and allow a greater degree of DOC processing during lateral transport (Olefeldt and Roulet, 2014, 2012; Tang et al., 2018; Walvoord and Striegl, 2007). For these reasons, coupled aquatic-soil studies of organic matter (OM) in continuous-discontinuous permafrost regions are needed (Vonk et al., 2019). The importance of surface waters from frozen peatlands in DOC processing and CO_2 emissions motivated numerous studies of aquatic

DOM (Hulatt et al., 2014; Manasypov et al., 2015; Mann et al., 2015, 2012; Peura et al., 2020; Pokrovsky et al., 2016; Shirokova et al., 2019). The latter study in NE European tundra peatlands demonstrated weak biodegradation of DOM along a hydrological continuum from peatland subsidence to a large river (Pechora) and suggested that CO_2 emission from surface waters could be explained either by sediment respiration or by fast processing of fresh supra-permafrost flow delivered from peat pore water and thawing soil ice. As such, to quantify overall DOM biodegradation potential in Arctic peatland waters, it is necessary to study the full continuum of surface fluids, from the soil and supra-permafrost waters to large lakes or river systems using universal techniques over large geographic coverage (Ma et al., 2019).

This study aimed to quantify the magnitude and controlling factors of DOM biodegradation potential along a hydrological continuum from soil water to medium-sized rivers and lakes located in a discontinuous permafrost area in western Siberia and northern Sweden. Strong seasonal variability in the high latitude C cycle is well known (Gao et al., 2019; Li et al., 2019). Yet, this study was carried out during baseflow period (July to October) when the quality and quantity of the DOC in waters are most stable (Chupakov et al., 2020; Holmes et al., 2012; Manasypov et al., 2015; Neff et al., 2006; Olefeldt and Roulet, 2012; Tang et al., 2018). Our working hypothesis is that the BDOC decreases along the HC (with the preferential degradation of easily biodegradable C molecules) and that the amplitude of this decrease depends on landscape context and the DOM origin. To test this hypothesis, we carried out aerobic biodegradation experiments (following Vonk et al. (2015)) and monitored resulting changes in DOM quantity and quality. We further compared the possible contribution of DOM biodegradation along the HC to published CO_2 emission from the surface waters representative of the study regions.

2. Materials and methods

2.1. Geographical, climatic and hydrological setting of sampling sites

In high latitude continental planes, the permafrost thaw leads to the formation of "thermokarst" (thaw) lakes resulting from the soil ice melt and the permafrost subsidence in frozen wetlands. The formation and development of thermokarst lakes appeared to follow a cycle (Kirpotin et al., 2009; Pokrovsky et al., 2011) and is an important part of the hydrological continuum of the region (Figure 1). The cycle starts with the subsidence of thawing soil forming a depression and filled by high molecular weight OM rich thaw water. The size of the depression grows due to the ongoing subsidence of peat soil and the active abrasion of edges until it reaches a lake size (thermokarst lake) with stable edges, that can be eventually drained into another lake or streams and rivers. The vegetation can then colonize the drained lake bottom and gradually the permafrost will be renewed, and the cycle can start over again by the formation of a wet depression. Lichens mostly dominate in mounds, while sphagnum type colonizes depressions, and graminoïds can be found in fens and drained lakes.

The two selected study sites are located in the artic/subarctic region, within a discontinuous permafrost area. Their detailed description can be found elsewhere (Åkerman and Johansson, 2008; Brown et al., 1997; Raudina et al., 2018). The Siberian study site (referred to as Khanymey, Figure S1 A in supplementary), is located near the town of Khanymey (63°47' N; 75°32' E) in a northern taiga, with a mean annual temperature of -5.6 °C and precipitation of 540 mm. The palsa peat bogs have a peat thickness of 0.1 to 1.4 m and the active (unfrozen) layer thickness (ALT) is around 90 and 215 cm under the surface of mounds and hollows, respectively. The vegetation on the mounds is dominated by dwarf shrubs (*Ledum* ssp., *Betula nana, Andromeda polifolia, Vaccinium* ssp., *Empetrum nigrum*), lichens (*Cladonia* ssp., *Cetraria, Ochrolechia*) and mosses, while the hollows are covered by moss-sedge associates (grasses *Eriophorum russeolum, E. vaginatum, Carex rotundata, C. limosa, Menyanthes*

trifoliate, Comarum palustre; mosses *Sphagnum. balticum, S. majus, S. lindbergii, S. warnstorfii*) and dwarf shrubs, such as *Oxycoccus palustris* (Raudina et al., 2018). In Khanymey, we have chosen seven locations that belonged to a HC. They were sampled in July 2018 and used as substrates for incubation. We sampled two supra-permafrost waters from peatland, one on a mound and one on a hollow (see sampling details in Raudina et al., 2018); two lakes: organic-rich Chernoe and organic-poor Trisino; two streams: the one close to the outlet of the lake and another one located far from this outlet (Lymbydyakha); and finally one medium-size river Pyakopur that flows through peatland and forest (Ala-aho et al., 2018). Localization, surface, depth and physicochemical parameters of the seven sampled locations are presented in the supplementary Table S1.

The second site is the Stordalen mire (68°21' N and 19°02' E) located in the vicinity of Abisko in Northern Sweden (Figure S1 B). The ALT in the mire is approximately 0.5 to 1 m thick (Åkerman and Johansson, 2008; Klaminder et al., 2008) and composed of 0.5 m of peat (Malmer et al., 2005) that overlays silty lacustrine sediment that has a glacial origin at depth (Klaminder et al., 2008). The mean annual temperature is -0.7 °C (Kohler et al., 2006) and the annual precipitation is 299 mm (Petrescu et al., 2007). The Stordalen mire is an ombrotrophic palsa that rises above semi-wet and wet minerotrophic fens, streams and shallow lakes (Wik et al., 2013). The hummock (*i.e.* the equivalent of mound structure in the Khanymey site) vegetation is dominated by lichens (*Cladonia* spp. and *Cetraria* spp. and mosses, such as *Sphagnum balticum* (Russ.) C. Jens.) in the bottom layer while *Eriophorum vaginatum* and *Empetrum hermaphroditum* dominated in the field layer. In the hollows, the field layer is dominated by graminoids such as *Carex rotundata, E. vaginatum* and *E. angustifolium* while the bottom layer consists of mosses, such as *S. balticum, S. fuscum* and carpet Bryatae (Malmer et al., 2005). Seven locations were sampled in the Stordalen mire in October 2018, before snowfall and ice-on: the soil solution of a hummock, the water from a crack at the edge of a

small pond, the small pond itself, a fen, a lake (Villasjön, Wik et al. (2013)) and two streams, a proximal one, near the outlet of the lake and a distal one located at the border of the mire. Localization, surface, depth and physicochemical parameters of the seven sampled locations are presented in Table S1. In the case of soil solution samples, a pit was made on hummock (/mound) or hollow. After a few minutes, gravitational (supra-permafrost) water from the surrounding soils was accumulated in the pit. This supra-permafrost water has been used for the experiment and named "soil solution" in the rest of this study.

2.2. Experimental setup

Each water sample was collected directly in a MilliQ-rinsed Nalgene® bottle and processed in less than 12 h after sampling following the protocol of Vonk et al. (2015) and Shirokova et al. (2019), employing the same filter units and membranes. All the manipulations were performed under sterile conditions. Waters collected in the field were first filtered through pre-combusted (4 hours at 450°C) GF/F filters (Whatman, nominal pore diameters: 0.7 µm, diameter 47 mm) using sterile filtration units (Millipore, 250 mL) and then incubated in sterile 60 mL amber glass bottles at 20 ± 2 °C, without light exposure. To keep oxygenic conditions in incubation bottles, bottle caps were not completely tightened and bottles were manually shaken at least every two days. Each sampling included filtration through pre-combusted GF/F filters mounted on a Sartorius filter unit (25 mm diameter). The duration of incubation depended on field logistics and ranged from 30 days in Siberian waters to 15 days in Northern Sweden. Information on sampling date, replicate and the type of conducted analyses are listed in Table S2.

2.3. Analyses

The pH (uncertainty of ± 0.01 pH units), conductivity (± 0.1 µS cm^{-1}) and absorbance (250 to 500 nm, 1 nm step; SpectraMax M5e Molecular Devices in Stordalen, and Eppendorf

BioSpectrometer® basic in Khanymey) were measured within 1 h after the sampling. Fixation and/or storage methods for each type of delayed analysis are listed in Table S2. Water samples for DOC and fluorescence analyses were adjusted around pH = 2 using HCl, which removed the dissolved inorganic carbon (DIC) and minimize the quenching of fluorescence caused by metal complexation (McKnight et al., 2001). Fluorescence was measured according to Roehm et al. (2009) on a SpectraMax M5e. DOC and DIC were measured by a high-temperature thermic oxidation method using a Shimadzu TOC-VSCN analyzer, with an uncertainty of 2%. Organic acids and anions were measured by high-performance ionic chromatography (Dionex Ics-5000^{+}). Total bacterial cells (TBC) concentration was measured by flow cytometry (Guava® EasyCyte^{TM} systems, Merck) using 1 µL of 10 times diluted SYBR GREEN (Merck) marker, added to 250 µL of each sample before analysis. The typical uncertainty on these measurements was between 10 and 20%.

2.4. Data treatment

The biodegradability of DOC (BDOC) was determined using commonly used equations proposed by Vonk et al. (2015) (Table S3). This gives the relative proportion of the biodegradable DOC in relation to the initial DOC concentration (Table S3). The apparent removal rate of DOC (RDOC) was calculated as the slope of linear regression for the incubation time (RDOC, Table S3). As the biodegradation of Khanymey and Stordalen did not last the same amount of time (respectively 30 and 15 days), in the rest of the article the RDOC and BDOC values were calculated at 15 days of incubations to allow a direct comparison between the two sites (*i.e.* $BDOC_{15}$ and $RDOC_{15}$). Absorbance data (Peacock et al., 2014; Weishaar et al., 2003) were used to assess the (*i*) the molecular weight of the DOC by the weight average molecular weight index (WAMW), (*ii*) the humification of DOM by the E2:E4 ratio and (*iii*) the relative amount of aromatic components by the specific UV absorbance at 254 nm

(SUVA$_{254}$) (Table S3). The Fluorescence index (FI) (McKnight et al., 2001), was calculated to separate DOC from a terrestrial origin (FI<1.4) than DOC from a microbial origin (FI > 1.4, Cory et al., 2010; Roehm et al., 2009) as detailed in Table S3.

Statistical treatment of the data included least-square linear regression and Pearson correlation to assess the evolution of parameters during incubation. To compare the biodegradation in waters within and between each HC principal component analysis (PCA) was used. Input data included initial chemical and biological parameters of waters that are hypothesized to contribute to the variation of $BDOC_{15}$ and $RDOC_{15}$ of waters: DOC, TBC, WAMW, E2:E4 ratio, pH, PO4-P, $SUVA_{254}$, conductivity and some organic acids concentrations (acetate, lactate and formate). The statistics were performed using R software (version 3.6.1) with "FactoMineR" and "factoextra" packages. All measured incubation parameters are provided in the Mendeley Data Repository (Payandi-Rolland, 2020).

3. Results

3.1 Inorganic water chemistry at the beginning of incubation

In Khanymey water at day 0 of incubation, the pH increased along the HC (from soil solution - mound at 4.2 to the Pyakopur river at 6.0). Specific conductivity ranged from 15 to 47 µS cm^{-1} in the proximal stream and in the soil solution sampled at the mound, respectively. The DIC concentration of all waters was lower than 1.1 mg L^{-1} (supplementary Table S1). In Stordalen, the pH of waters increased along the HC (from 4.1 at the crack to 7.2 at the distal stream and Villasjön Lake). The specific conductivity ranged from 26 to 100 µS cm^{-1} in the fen and in the soil solution from the hummock, respectively. The DIC concentrations ranged from 1.7 (small pond) to 4.6 mg L^{-1} (proximal stream; supplementary Table S1).

227 *3.2 Biodegradation of DOC*

228 The DOC concentration of the Khanymey site showed high initial DOC values for
229 waters located at the beginning of the HC (*i.e.* soil solution at the mound and hollow, and the
230 Lake Chernoe, Figure 2 A.1). The DOC concentrations at the end of HC (*i.e.* lake Trisino,
231 proximal and distal stream, and the Pyakopur River) were much lower and ranged between 14.5
232 and 16.7 mg L^{-1}. The DOC concentrations showed a significant linear decrease ($p < 0.05$, R^2
233 ranging between 0.45 to 0.69) in all incubations, except for the soil solution from the hollow
234 and both thermokarst lakes (Figure 2 A.1). The corresponding BDOC value increased in all
235 incubations from day 0 to 30 (Figure 2 B.1). After 15 days of the experiment, the lowest
236 $BDOC_{15}$ value was -0.4 ± 2.3% for the soil solution from the mound and the highest was 21.9
237 ± 4.9% for the Trisino Lake (Figure 3). The rates of DOC removal over 15 days ($RDOC_{15}$) with
238 the highest rates in the soil solution from the hollow (0.61 ± 0.1 mg L^{-1} d^{-1}), and the lowest in
239 lake Chernoe (-0.11 ± 0.1 mg L^{-1} d^{-1}) (Figure 3 and Table S5). Soil solution from the mound
240 exhibited the highest concentration of low molecular weight organic acids (LMWOA), *i.e*.
241 formate, lactate and acetate (Table S4). Initial values of bacterial cell numbers (TBC) ranged
242 from 2.89×10^5 (Trisino Lake) to 1.43×10^6 cells mL^{-1} (distal stream) (Table S1). During the
243 incubation, the bacterial concentration increased by 30% of the initial amount in the soil
244 solution from the mound to 72% in the incubation of the distal stream (data not shown).

245 The DOC concentrations in the Stordalen waters were high at the beginning of the
246 continuum (soil solution, hummock and crack), then decreased in the small pond, and became
247 lower at the end of the continuum (fen, Villasjön Lake, proximal and distal stream) (Figure 2
248 A.2). The DOC concentrations significantly decreased during incubations. The corresponding
249 BDOC values increased in all incubations from day 0 to 15 (Figure 2 B.2). The $BDOC_{15}$ ranged
250 between 10.5 - 19.9% with the lowest values in the proximal stream and the crack, and the
251 highest in the distal stream (Figure 3). The waters located at the beginning of the continuum

exhibited the highest $RDOC_{15}$ while the lower $RDOC_{15}$ values were observed for end-members of the HC (Figure 3 and Table S5). As for the Khanymey continuum, soil solution from the hummock contained much higher initial concentrations of acetate and formate compared with other incubated waters (Table S4). During incubation, only the soil solution from the hummock showed a decrease (78%) in acetate concentrations. The initial TBC ranged from 2.26×10^3 (distal stream) to 3.76×10^4 cells mL^{-1} (crack) (Table S1). During the incubation period, the lowest increase in TBC was obtained for the Villasjön Lake (49%) and the highest increase was measured for the distal stream (by a factor of 25, data not shown).

3.3 DOM optical properties

In the Khanymey continuum, the $SUVA_{254}$ ranged between 3.4 L mg C^{-1} m^{-1} for the proximal stream to 4.2 L mg C^{-1} m^{-1} for the river (Figure 2 C.1). The $SUVA_{254}$ increased in all samples during the incubations, with the lowest increase for the soil solution – mound (14%) and highest for the proximal stream (60%). The ratio E2:E4 increased with incubation time at the beginning of the continuum (both soil solutions and the Chernoe Lake) and decreased with time in waters located at the end of HC (from the Trisino lake to the Pyakopur River) (Figure S2 A.1). Normalized molecular weight (WAMW) allowed distinguishing 2 groups of samples (Figure S2 B.1). The first one included soil solutions from the mound and hollow and the Chernoe Lake, with stable values ranging between 516 - 526 and 526 - 540 Da from the beginning to the end of the incubation, respectively. The second group comprised all other water types of the continuum, with WAMW values increasing from 558 - 586 Da to 590 - 679 Da during the incubations.

In the Stordalen hydrological continuum, the $SUVA_{254}$ ranged between 2.9 and 4.9 L mg C^{-1} m^{-1} at the beginning to 3.3 and 5.1 L mg C^{-1} m^{-1} at the end of the experiment (Figure 2 C.2). An increase in $SUVA_{254}$ of 12, 19 and 22% was observed during the incubation of the soil

277 solution – hummock, proximal and distal stream. For the remaining samples of the Stordalen
278 continuum, the increase in $SUVA_{254}$ was below 10%. The evolution of the ratio E2:E4 during
279 incubations separated the systems in two groups (Figure S2 A.2), i.e. one with stable values at
280 the beginning of the HC (*i.e.* crack, small pond, fen, and soil solution), and one with oscillating
281 values at the end of the HC (*i.e.* both streams and the lake). The lowest WAMW values were
282 recorded for soil solution - hummock and crack with the initial and final values of 506-511 and
283 513-515 Da, respectively (Figure S2 B.2). The highest values of WAMW were obtained for the
284 small pond and the proximal stream (initial: 625 to 716 Da, final: 662 to 779 Da). The
285 fluorescence index (FI) of waters in the Stordalen HC ranged between 1.52 and 2.23 at the
286 beginning of incubation for the crack and the distal stream, respectively (Figure 2 D). FI values
287 decreased for all waters during incubation, with values < 1.40 for the crack, the small pond and
288 the fen and slightly higher values for the proximal stream (1.67 ± 0.2) after 5 days of incubation.
289
290 *3.4 PCA results*
291 The principal component analysis (PCA) performed on data from both hydrological
292 continuums (Figure 4 and Table S6) showed that the component number 1 (PC1) explained
293 34.0% of the variation, with an important contribution of conductivity, DOC concentration,
294 $RDOC_{15}$ and organic acids concentrations (acetate and formate). The PC2 explained 26.9% of
295 the variations, with the largest contribution coming from E2:E4 ratio, $SUVA_{254}$, pH and
296 LMWOA concentration. The $BDOC_{15}$ appeared to be grouped with the pH and the E2:E4 ratio,
297 whereas lactate, DOC, and $SUVA_{254}$ were on the opposite side of the plot. Acetate and formate
298 concentrations and specific conductivity were grouped tight. No clear visual separation by study
299 site could be seen. However, the end-member waters of both continuums were clustered in the
300 upper left quadrant of the plot, while other waters, except the soil solution from the mound of
301 Khanymey, were mostly located in the lower right quadrant.
302

4. Discussion

4.1 Evolution of the DOC removal rate and biodegradability along the hydrological continuum

The decreasing trend of $RDOC_{15}$ values observed along the HC, and the inverse trend for $BDOC_{15}$ values (Figure 3) suggest that the soil waters located at the beginning of the continuum contain rapidly processed DOC, while the lake and river waters, at the end of HC, contain slowly processed DOC. Drastic differences in $RDOC_{15}$ between the beginning and the end of the HC suggest that these changes across pore waters, supra-permafrost waters, surface small ponds and depressions of frozen peatlands, are primarily controlled by water residence time (Catalán et al., 2016; Obernosterer and Benner, 2004). Indeed, when the residence time of water is short, the decay rate of OC is believed to be governed by photo-degradation and flocculation of OC (Catalán et al., 2016; Evans et al., 2017). Moreover, the labile parts of the DOM are likely to be firstly processed during the transition because the fresher DOC is delivered into the early stages of the HC.

The $BDOC_{15}$ of streams and rivers in both continuums ranged between 10 to 20% (Figure 3) which is generally consistent with the values obtained for Arctic riverine systems (typically 10 to 40%, Holmes et al., 2008; Mann et al., 2012; Wickland et al., 2012) and for waters of thawing and collapsing permafrost (10 to 40%, Abbott et al., 2014). Soil solutions, crack, small pond, fen and lake waters had a $BDOC_{15}$ ranging between 0 and 20%, which is consistent with the biodegradability of lake waters from the Stordalen mire (10 to 20%, Roehm et al., 2009). However, the biodegradability of fen leachate in the latter study ranged between 50 and 60%, which is 4 times higher than our values for the fen (~15%). Presumably, the fresh leachate used by Roehm et al. (2009) contained a higher concentration of bioavailable OM compared with natural, partially processed, fen waters used in this and other studies (*i.e.* Michaelson et al., 1998; Spencer et al., 2015; Wickland et al., 2007). The $BDOC_{15}$ values across

328 the two continuums of this study are at the highest range of those reported in the HC of frozen
329 peatlands of Northern Eurasia (between 0 to 10% for depression, thermokarst lake, river and
330 stream, Shirokova et al., 2019) and also slightly higher than the BDOC of waters from
331 discontinuous permafrost (5 to 15%, mean 14%) (Vonk et al., 2015).

332 The PCA analysis allowed distinguishing two trends of biodegradability behavior linked
333 to LMWOA: *i*) the $BDOC_{15}$, which negatively correlated with lactate but was not linked to
334 acetate and formate, and *ii*) the $RDOC_{15}$; positively correlated to acetate and formate but which
335 did not correlate with lactate. This could suggest that the initial concentration of acetate and
336 formate influences the removal rate of DOC, because their presence triggers intensive microbial
337 metabolism as it was also observed by Cappenberg et al. (1982). In contrast, the overall
338 biodegradability of waters may be linked to the pattern of lactate which dominated in
339 concentrations of LMWOA of both continuums.

340

341 *4.2 Evolution of the DOC quality along the hydrological continuum*

342 The positive and negative correlation between E2:E4 spectral ratio and $SUVA_{254}$
343 respectively, with $BDOC_{15}$ observed by the PCA analysis (Figure 4), implies that an increase
344 in the humification of DOM and a decrease in the concentration of aromatic components
345 increase the biodegradable potential of DOM. The grouping of individuals waters located at the
346 end of both continuums in the upper left quadrant of the PCA biplot suggests that they are
347 influenced by the same variables (WAMW, TBC, pH and E2:E4 ratio). This is not observed for
348 waters at the beginning of continuums, whose signals were widely spread on the biplot. Such a
349 grouping of waters can be due to the mixing of large water bodies, receiving mostly lateral
350 surface flow due to precipitation, while smaller water bodies are mainly supplied by lateral
351 surface and supra-permafrost flow from thawing permafrost (Figure 1).

For the Stordalen continuum, a decreasing trend of FI in the course of incubation of each water of the HC (Figure 2 D) indicates either *i*) an increase in the terrestrially-derived OM or *ii*) a decrease in the microbially-derived OM (Cory et al., 2010; Mann et al., 2012). As no fresh vegetation leachate was added in our incubations, the observed decrease of FI values during the incubation of Stordalen waters corresponds to a relative decrease in the amount of microbially-derived OM compared to the overall amount of OM. This is at odds with the reported resistance of the bacterially-derived OM to the microbial degradation in freshwater (Kawasaki et al., 2013). We, therefore, hypothesize that the relative decrease of the microbially-derived OM occurred due to a lack of easily biodegradable terrestrial OM and the persistence of the most recalcitrant part of terrestrial OM, which is consistent with an increase in $SUVA_{254}$ and WAMW with the incubation time. Moreover, a recent study on the evolution of the DOM along a soil-stream-river continuum (Hutchins et al., 2017) demonstrated that soil-stream waters were a hot spot of DOM degradation, with selective removal of low molecular weight (LMW) components, whereas stream-river waters were more dominated by the degradation of humic-like aromatic components. This trend is also observed in our study, particularly for the Khanymey continuum in which the E2:E4 ratio (a proxy for humification degree) increased during incubation of waters located at the beginning of the HC and decreased with time for the waters at the end of the HC (Figure S2 A.1). This is also in agreement with the rapid uptake of LMWOA observed during incubation (Table S4). $SUVA_{254}$ of the Khanymey and Stordalen HC (up to 6.3 and 5.5 L mg C^{-1} m^{-1}, respectively) are greater than most of the previously reported data of waters from depressions, lakes and river of discontinuous permafrost area (3.3 to 4.4 L mg C^{-1} m^{-1} (Roehm et al., 2009; Shirokova et al., 2019), but comparable to the values of permafrost leachate (6.6 ± 0.1 L mg C^{-1} m^{-1}, Roehm et al.; 2009). Such high SUVA values reflect the dominance of allochthonous DOM of peat, providing the majority of DOC input to the water bodies.

4.3 Comparison between the hydrological continuum of Khanymey and Stordalen

We note that there are somewhat higher levels of $BDOC_{15}$ in waters from the Stordalen peat mire compared with the Khanymey peatlands (10 to 20% and 0 to 20%, respectively, Figure 3). This difference cannot be attributed to the difference in seasons of sampling (July in Khanymey and October in Stordalen) because, even if seasons are known to play an import role in the BDOC, it has been shown that BDOC generally decreases as the Arctic summer progress (Holmes et al., 2008; Mann et al., 2012; Vonk et al., 2015; Wickland et al., 2012). Therefore, the effect of seasons would produce an opposite effect to that observed in this study. Moreover, the PCA revealed that the $BDOC_{15}$ is not correlated to the TBC (Figure 4). Thus, given the higher values of $BDOC_{15}$ and the lower values of TBC in Stordalen compared with Khanymey, we hypothesize that the biodiversity of microorganisms in the experiment, rather than the microbial number (TBC) impact the final BDOC of waters. It has been shown that the microbial community drastically and rapidly changes between summer and winter period with a syntrophic winter community having a higher potential for mobilizing and converting complex organic matter to more labile C sources (Vigneron et al., 2019). Consistent with this observation, our results show a smaller increase in the $SUVA_{254}$ (reflecting the presence of aromatic components, Hood et al. (2005); Neff et al. (2006)) during incubation of waters from Stordalen (12 to 22% increase) compared to Khanymey (14 to 58% increase) (Figure 2 C). In comparison, the biodegradation of peat water from the European boreal zone using the experimental approach similar to that of the present study, produced an increase in $SUVA_{254}$ by 7.4 ± 4.2 % (Hulatt et al., 2014).

4.4 How does CO_2 production from experimental DOC biodegradation relate to field-based fluxes estimates

The findings of this study and widely reported dominance of low-biodegradable DOC (0-15% BDOC) in large rivers and streams of the discontinuous permafrost zone (Frey et al., 2016; Vonk et al., 2015) suggest that 1) the majority of DOC is degraded before its arrival to large aquatic reservoirs (Striegl et al., 2005), and 2) the CO_2 supersaturation and emission of surface waters of frozen peatlands can be largely a result of soil, soil pore water and sediment respiration rather than an aerobic bio- and photo-degradation of DOM in the water column (Audry et al., 2011; Deshpande et al., 2017; Rocher-Ros et al., 2020; Shirokova et al., 2019).

In order to quantify the potential importance of biodegradation of DOC to the atmospheric CO_2 fluxes from the study systems, we assumed that the entire consumed DOC was converted into CO_2. This assumption allows to determine the maximal CO_2 emission possible due to the biodegradation, keeping in mind that the true value is likely lower. Thus, to assess the amount of CO_2, potentially emitted due to the total mineralization of OC *via* biodegradation (RCO_2) in each water body, we multiplied $RDOC_{15}$ (Table S5) by the mean depth of the water columns (Table S1). This calculation assumes 1) negligible uptake of C for bacterial biomass growth, 2) constant biodegradation intensity over the full depth of the water column, and that 3) the entire DOC pool is available for degradation. The obtained RCO_2 values decreased for both HC from headwaters to streams and rivers of both Khanymey (range: -33 ± 45 to 241 ± 72 mg C-CO_2 m^{-2} d^{-1}) and the Stordalen (9 ± 3 to 359 ± 63 mg C-CO_2 m^{-2} d^{-1}) HC (Figure 5). The median (± IQR) RCO_2 values of thaw ponds and lakes of the Khanymey site (169 ± 72 mg C-CO_2 m^{-2} d^{-1}, data not shown) are sizably lower than the median CO_2 emissions from the western Siberia lowland (WSL) thermokarst lakes measured by floating chambers (1,101 ± 4,150 mg C-CO_2 m^{-2} d^{-1}, Serikova et al. (2019)). The RCO_2 of the Khanymey streams and river (49 ± 68 mg C-CO_2 m^{-2} d^{-1}, data not shown) are also much lower than the median

values of CO_2 emissions from the WSL rivers (6,000 ± 3,900 mg C-CO_2 m^{-2} d^{-1}, Serikova et al. (2018)). Similarly, the median RCO_2 of pond, fen and lake of the Stordalen site (38 ± 62 mg C-CO_2 m^{-2} d^{-1}, data not shown) are much lower than the median CO_2 emissions from small (4-150 m^2) thaw ponds of this mire (3,348 ± 1,392 mg C-CO_2 m^{-2} d^{-1}, Kuhn et al. (2018)). This comparison clearly demonstrates that the potential contribution of DOC biodegradation to the field-measured CO_2 emissions from inland waters of permafrost peatlands is typically below 10 % (Figure 5).

Therefore, the DOC biodegradation rates obtained in this study for the water column appear to be insufficient to support the observed CO_2 emissions from the water surface to the atmosphere. Several factors can contribute to this disparity. First, aerobic and anaerobic respiration of stream, lake and river sediments as well as soil water input *via* supra-permafrost flow (i.e., Raudina et al., 2018), that can produce a sizeable amount of CO_2, thus increasing overall C emission potential of the aquatic systems (MacIntyre et al., 2018; Valle et al., 2018). For example, anaerobic C mineralization of thermokarst lake sediments is fairly well established in discontinuous permafrost zone of peat bogs in western Siberia (Audry et al., 2011) and Canada (Deshpande et al., 2017). Second, the photo-degradation (Panneer Selvam et al., 2019) of OM as well as the photo-stimulation of the microbial respiration, which is known to decrease along the HC (Cory and Kling, 2018), could enhance natural CO_2 emission compared to laboratory incubations. Third, the POC present in the water column in the field can sizably contribute to overall CO_2 emissions from surface waters: it has been shown that, during laboratory incubations of boreal and subarctic waters, the POC is 15 times more reactive towards biodegradation than DOC (Attermeyer et al., 2018).

Our study dealt solely with dissolved components in closed systems and was conducted in the ice-free season of arctic peatlands. Although the results of both incubations are comparable between sites, which were sampled during the baseflow summer-autumn period,

additional factors need to be considered in order to fully understand the biogeochemical processing of organic carbon in natural systems. These include i) seasonality (Gao et al., 2019; Kaiser et al., 2017; Li et al., 2019), notably spring snowmelt period (Tang et al., 2018) and potential anoxic conditions in summer and winter (Deshpande et al., 2017), ii) water retention time (Moore, 2009; Olefeldt and Roulet, 2012; Tang et al., 2018), iii) vegetation cover which affects quality and quantity of OM input (Gałka et al., 2017; Kaiser et al., 2017); iv) the ratio of water volume to soil/sediment surface area which determines the rate of fresh OM input (Polishchuk et al., 2017), v) the biodegradability of the particulate organic carbon (Attermeyer et al., 2018), and vi) redox conditions in the water column (Deshpande et al., 2017) and at the water-sediment interface (Valle et al., 2018).

5. Conclusions

Biodegradation experiments demonstrated a decreasing trend of DOC removal rate along the HC from soil solutions to lakes, streams, and rivers of the discontinuous permafrost zone of permafrost peatlands of W. Siberia and N. Sweden. While we hypothesized a decrease of the DOC biodegradability along the HC, the BDOC increased from the beginning to the end of the continuum. This could be linked to preferential removal of labile, low molecular weight compartments of the DOM which are likely to be firstly processed during the transition because the fresher DOC is delivered into the early stages of the HC. Low DOM biodegradability reported in this study (0 and 20%) suggests that the majority of BDOC is degraded before its arrival to a larger aquatic reservoir or even before reaching surface waters. We also suggest that the biodegradation can support part of the CO_2 emissions from surface waters of these peatlands but that other sources are likely of larger importance, including soil and sediment respiration of dissolved and particulate OC, photo-degradation and photo-stimulation of the microbial respiration. Concurrent measurements of BDOC and direct CO_2 emissions in the field are needed to constrain the quantitative importance of *in-situ* DOM degradation for CO_2 fluxes to the atmosphere. Considering the fast processing of OM at the beginning of the continuum and the increasing biodegradability of waters along the HC, this study highlights the importance of accounting for the large spatial heterogeneity of aquatic environments which is needed for mechanistically modeling of C cycling in permafrost peatlands.

CRediT authorship contribution statement

D. Payandi-Rolland: conceptualization, investigation, writing – original draft, **L.S. Shirokova**: conceptualization, investigation, writing – original draft, **M. Tesfa**: investigation, **P. Bénézeth**: writing – original draft, **A.G. Lim**: investigation, **D. Kuzmina**: investigation, **J. Karlsson**: conceptualization, writing – original draft, **R. Giesler**: conceptualization, writing – original draft, **O.S. Pokrovsky**: conceptualization, writing – original draft.

Acknowledgments

The fieldwork in Siberia was supported by the international program INTERACT for the 2018 campaign ("BIOCARSIB"), the Russian Fund for Basic Research grant no. 19-29-05209-mk, and Russian Scientific Fund project No 18-77-10045 (fieldwork in Khanymey). The fieldwork in Sweden was supported by the international project for mobility funded by the University Paul Sabatier (Toulouse 3, France) ("BioCarZA") and by the Swedish Research Council (grant no. 2016-05275). **D.P-R** was supported by a Ph. D. fellowship from the French « Ministère de l'Enseignement Supérieur, de la Recherche et de l'Innovation ». **M.T** was supported by the « Axe transverse – AST GES » of the Observatoire Midi-Pyrénées. We thank our colleagues from the Tomsk State University (TSU) for the logistic and help during the Siberian field trip. We thank the Climate Impacts Research Centre (CIRC), Umeå University, for hosting the Swedish experimental part of this research. We are grateful to Carole Causserand (GET) for help with DIC and DOC concentrations analyses, Frédéric Julien (EcoLab) for Dionex HPLC measurements of anions and organic acids, and Joey Allen (Ecolab) as well as Joséphine Leflaive (Ecolab) for the help on flow cytometry.

Conflicts of interests

The authors declare no conflict of interest.

References

Abbott, B.W., Jones, J.B., Schuur, E.A.G., III, F.S.C., Bowden, W.B., Bret-Harte, M.S., Epstein, H.E., Flannigan, M.D., Harms, T.K., Hollingsworth, T.N., Mack, M.C., McGuire, A.D., Natali, S.M., Rocha, A.V., Tank, S.E., Turetsky, M.R., Vonk, J.E., Wickland, K.P., Aiken, G.R., Alexander, H.D., Amon, R.M.W., Benscoter, B.W., Bergeron, Y., Bishop, K., Blarquez, O., Bond-Lamberty, B., Breen, A.L., Buffam, I., Cai, Y., Carcaillet, C., Carey, S.K., Chen, J.M., Chen, H.Y.H., Christensen, T.R., Cooper, L.W., Cornelissen, J.H.C., Groot, W.J. de, DeLuca, T.H., Dorrepaal, E., Fetcher, N., Finlay, J.C., Forbes, B.C., French, N.H.F., Gauthier, S., Girardin, M.P., Goetz, S.J., Goldammer, J.G., Gough, L., Grogan, P., Guo, L., Higuera, P.E., Hinzman, L., Hu, F.S., Hugelius, G., Jafarov, E.E., Jandt, R., Johnstone, J.F., Karlsson, J., Kasischke, E.S., Kattner, G., Kelly, R., Keuper, F., Kling, G.W., Kortelainen, P., Kouki, J., Kuhry, P., Laudon, H., Laurion, I., Macdonald, R.W., Mann, P.J., Martikainen, P.J., McClelland, J.W., Molau, U., Oberbauer, S.F., Olefeldt, D., Paré, D., Parisien, M.-A., Payette, S., Peng, C., Pokrovsky, O.S., Rastetter, E.B., Raymond, P.A., Raynolds, M.K., Rein, G., Reynolds, J.F., Robards, M., Rogers, B.M., Schädel, C., Schaefer, K., Schmidt, I.K., Shvidenko, A., Sky, J., Spencer, R.G.M., Starr, G., Striegl, R.G., Teisserenc, R., Tranvik, L.J., Virtanen, T., Welker, J.M., Zimov, S., 2016. Biomass offsets little or none of permafrost carbon release from soils, streams, and wildfire: an expert assessment. Environ. Res. Lett. 11, 034014. https://doi.org/10.1088/1748-9326/11/3/034014

Abbott, B.W., Larouche, J.R., Jones, J.B., Bowden, W.B., Balser, A.W., 2014. Elevated dissolved organic carbon biodegradability from thawing and collapsing permafrost: Permafrost carbon biodegradability. J. Geophys. Res. Biogeosciences 119, 2049–2063. https://doi.org/10.1002/2014JG002678

Åkerman, H.J., Johansson, M., 2008. Thawing permafrost and thicker active layers in sub-arctic Sweden. Permafr. Periglac. Process. 19, 279–292. https://doi.org/10.1002/ppp.626

Ala-aho, P., Soulsby, C., Pokrovsky, O.S., Kirpotin, S.N., Karlsson, J., Serikova, S., Manasypov, R., Lim, A., Krickov, I., Kolesnichenko, L.G., Laudon, H., Tetzlaff, D., 2018. Permafrost and lakes control river isotope composition across a boreal Arctic transect in the Western Siberian lowlands. Environ. Res. Lett. 13, 034028. https://doi.org/10.1088/1748-9326/aaa4fe

Attermeyer, K., Catalán, N., Einarsdottir, K., Freixa, A., Groeneveld, M., Hawkes, J.A., Bergquist, J., Tranvik, L.J., 2018. Organic Carbon Processing During Transport Through Boreal Inland Waters: Particles as Important Sites. J. Geophys. Res. Biogeosciences. https://doi.org/10.1029/2018JG004500

Audry, S., Pokrovsky, O.S., Shirokova, L.S., Kirpotin, S.N., Dupré, B., 2011. Organic matter mineralization and trace element post-depositional redistribution in Western Siberia thermokarst lake sediments. Biogeosciences 8, 3341–3358. https://doi.org/10.5194/bg-8-3341-2011

Brown, J., Ferrians Jr, O., Heginbottom, J., Melnikov, E., 1997. Circum-Arctic map of permafrost and ground-ice conditions. US Geological Survey Reston, VA.

Cappenberg, T.E., Hordijk, K.A., Jonkheer, G.J., Lauwen, J.P.M., 1982. Carbon flow across the sediment-water interface in Lake Vechten, The Netherlands. Hydrobiologia 91, 161–168. https://doi.org/10.1007/BF02391932

Catalán, N., Marcé, R., Kothawala, D.N., Tranvik, L.J., 2016. Organic carbon decomposition rates controlled by water retention time across inland waters. Nat. Geosci. 9, 501–504. https://doi.org/10.1038/ngeo2720

Chapin, F.S., Woodwell, G.M., Randerson, J.T., Rastetter, E.B., Lovett, G.M., Baldocchi, D.D., Clark, D.A., Harmon, M.E., Schimel, D.S., Valentini, R., Wirth, C., Aber, J.D., Cole, J.J., Goulden, M.L., Harden, J.W., Heimann, M., Howarth, R.W., Matson, P.A., McGuire, A.D., Melillo, J.M., Mooney, H.A., Neff, J.C., Houghton, R.A., Pace, M.L., Ryan, M.G., Running, S.W., Sala, O.E., Schlesinger, W.H., Schulze, E.-D., 2006. Reconciling Carbon-cycle Concepts, Terminology, and Methods. Ecosystems 9, 1041–1050. https://doi.org/10.1007/s10021-005-0105-7

Chupakov, A.V., Pokrovsky, O.S., Moreva, O.Y., Shirokova, L.S., Neverova, N.V., Chupakova, A.A., Kotova, E.I., Vorobyeva, T.Y., 2020. High resolution multi-annual riverine fluxes of organic carbon, nutrient and trace element from the largest European Arctic river, Severnaya Dvina. Chem. Geol. 538, 119491. https://doi.org/10.1016/j.chemgeo.2020.119491

Cole, J.J., Prairie, Y.T., Caraco, N.F., McDowell, W.H., Tranvik, L.J., Striegl, R.G., Duarte, C.M., Kortelainen, P., Downing, J.A., Middelburg, J.J., Melack, J., 2007. Plumbing the Global Carbon Cycle: Integrating Inland Waters into the Terrestrial Carbon Budget. Ecosystems 10, 172–185. https://doi.org/10.1007/s10021-006-9013-8

Cory, R.M., Kling, G.W., 2018. Interactions between sunlight and microorganisms influence dissolved organic matter degradation along the aquatic continuum. Limnol. Oceanogr. Lett. 3, 102–116. https://doi.org/10.1002/lol2.10060

Cory, R.M., Miller, M.P., McKnight, D.M., Guerard, J.J., Miller, P.L., 2010. Effect of instrument-specific response on the analysis of fulvic acid fluorescence spectra. Limnol. Oceanogr. Methods 8, 67–78. https://doi.org/10.4319/lom.2010.8.67

Creed, I.F., McKnight, D.M., Pellerin, B.A., Green, M.B., Bergamaschi, B.A., Aiken, G.R., Burns, D.A., Findlay, S.E.G., Shanley, J.B., Striegl, R.G., Aulenbach, B.T., Clow, D.W., Laudon, H., McGlynn, B.L., McGuire, K.J., Smith, R.A., Stackpoole, S.M., 2015. The river as a chemostat: fresh perspectives on dissolved organic matter flowing down the river continuum. Can. J. Fish. Aquat. Sci. 72, 1272–1285. https://doi.org/10.1139/cjfas-2014-0400

Demars, B.O.L., 2019. Hydrological pulses and burning of dissolved organic carbon by stream respiration. Limnol. Oceanogr. 64, 406–421. https://doi.org/10.1002/lno.11048

Deshpande, B.N., Maps, F., Matveev, A., Vincent, W.F., 2017. Oxygen depletion in subarctic peatland thaw lakes. Arct. Sci. 3, 406–428. https://doi.org/10.1139/as-2016-0048

Evans, C.D., Futter, M.N., Moldan, F., Valinia, S., Frogbrook, Z., Kothawala, D.N., 2017. Variability in organic carbon reactivity across lake residence time and trophic gradients. Nat. Geosci. 10, 832–835. https://doi.org/10.1038/ngeo3051

Frey, K.E., Sobczak, W.V., Mann, P.J., Holmes, R.M., 2016. Optical properties and bioavailability of dissolved organic matter along a flow-path continuum from soil pore waters to the Kolyma River mainstem, East Siberia. Biogeosciences 13, 2279–2290. https://doi.org/10.5194/bg-13-2279-2016

Gao, T., Kang, S., Chen, R., Zhang, Taigang, Zhang, Tingjun, Han, C., Tripathee, L., Sillanpää, M., Zhang, Y., 2019. Riverine dissolved organic carbon and its optical properties in a permafrost region of the Upper Heihe River basin in the Northern Tibetan Plateau. Sci. Total Environ. 686, 370–381. https://doi.org/10.1016/j.scitotenv.2019.05.478

Holmes, R.M., McClelland, J.W., Peterson, B.J., Tank, S.E., Bulygina, E., Eglinton, T.I., Gordeev, V.V., Gurtovaya, T.Y., Raymond, P.A., Repeta, D.J., Staples, R., Striegl, R.G., Zhulidov, A.V., Zimov, S.A., 2012. Seasonal and Annual Fluxes of Nutrients

and Organic Matter from Large Rivers to the Arctic Ocean and Surrounding Seas. Estuaries Coasts 35, 369–382. https://doi.org/10.1007/s12237-011-9386-6
Holmes, R.M., McClelland, J.W., Raymond, P.A., Frazer, B.B., Peterson, B.J., Stieglitz, M., 2008. Lability of DOC transported by Alaskan rivers to the Arctic Ocean. Geophys. Res. Lett. 35. https://doi.org/10.1029/2007GL032837
Hood, E., Williams, M.W., McKnight, D.M., 2005. Sources of dissolved organic matter (DOM) in a Rocky Mountain stream using chemical fractionation and stable isotopes. Biogeochemistry 74, 231–255. https://doi.org/10.1007/s10533-004-4322-5
Hulatt, C.J., Kaartokallio, H., Asmala, E., Autio, R., Stedmon, C.A., Sonninen, E., Oinonen, M., Thomas, D.N., 2014. Bioavailability and radiocarbon age of fluvial dissolved organic matter (DOM) from a northern peatland-dominated catchment: effect of land-use change. Aquat. Sci. 76, 393–404. https://doi.org/10.1007/s00027-014-0342-y
Hutchins, R.H.S., Aukes, P., Schiff, S.L., Dittmar, T., Prairie, Y.T., Giorgio, P.A. del, 2017. The Optical, Chemical, and Molecular Dissolved Organic Matter Succession Along a Boreal Soil-Stream-River Continuum. J. Geophys. Res. Biogeosciences 122, 2892–2908. https://doi.org/10.1002/2017JG004094
Kawasaki, N., Komatsu, K., Kohzu, A., Tomioka, N., Shinohara, R., Satou, T., Watanabe, F.N., Tada, Y., Hamasaki, K., Kushairi, M.R.M., Imai, A., 2013. Bacterial Contribution to Dissolved Organic Matter in Eutrophic Lake Kasumigaura, Japan. Appl. Environ. Microbiol. 79, 7160–7168. https://doi.org/10.1128/AEM.01504-13
Kirpotin, S.N., Berezin, A., Bazanov, V., Polishchuk, Y., Vorobiov, S., Mironycheva-Tokoreva, N., Kosykh, N., Volkova, I., Dupre, B., Pokrovsky, O., Kouraev, A., Zakharova, E., Shirokova, L., Mognard, N., Biancamaria, S., Viers, J., Kolmakova, M., 2009. Western Siberia wetlands as indicator and regulator of climate change on the global scale. Int. J. Environ. Stud. 66, 409–421. https://doi.org/10.1080/00207230902753056
Klaminder, J., Yoo, K., Rydberg, J., Giesler, R., 2008. An explorative study of mercury export from a thawing palsa mire. J. Geophys. Res. Biogeosciences 113. https://doi.org/10.1029/2008JG000776
Kohler, J., Brandt, O., Johansson, M., Callaghan, T., 2006. A long-term Arctic snow depth record from Abisko, northern Sweden, 1913–2004. Polar Res. 25, 91–113. https://doi.org/10.3402/polar.v25i2.6240
Kuhn, M., Lundin, E.J., Giesler, R., Johansson, M., Karlsson, J., 2018. Emissions from thaw ponds largely offset the carbon sink of northern permafrost wetlands. Sci. Rep. 8, 9535. https://doi.org/10.1038/s41598-018-27770-x
Li, Y., Song, G., Massicotte, P., Yang, F., Li, R., Xie, H., 2019. Distribution, seasonality, and fluxes of dissolved organic matter in the Pearl River (Zhujiang) estuary, China. Biogeosciences 16, 2751–2770. https://doi.org/10.5194/bg-16-2751-2019
Lindström, M., Bax, G., Dinger, M., Dworatzek, M., Erdtmann, W., Fricke, A., Kathol, B., 1985. Geology of a part of the Torneträsk section of the Caledonian front, northern Sweden.
Liu, F., Kou, D., Abbott, B.W., Mao, C., Chen, Y., Chen, L., Yang, Y., 2019. Disentangling the Effects of Climate, Vegetation, Soil and Related Substrate Properties on the Biodegradability of Permafrost-Derived Dissolved Organic Carbon. J. Geophys. Res. Biogeosciences 124, 3377–3389. https://doi.org/10.1029/2018JG004944
Ma, Q., Jin, H., Yu, C., Bense, V.F., 2019. Dissolved organic carbon in permafrost regions: A review. Sci. China Earth Sci. 62, 349–364. https://doi.org/10.1007/s11430-018-9309-6
MacIntyre, S., Cortés, A., Sadro, S., 2018. Sediment respiration drives circulation and production of CO2 in ice-covered Alaskan arctic lakes. Limnol. Oceanogr. Lett. 3, 302–310. https://doi.org/10.1002/lol2.10083

Malmer, N., Johansson, T., Olsrud, M., Christensen, T.R., 2005. Vegetation, climatic changes and net carbon sequestration in a North-Scandinavian subarctic mire over 30 years. Glob. Change Biol. 11, 1895–1909. https://doi.org/10.1111/j.1365-2486.2005.01042.x

Manasypov, R.M., Vorobyev, S.N., Loiko, S.V., Kritzkov, I.V., Shirokova, L.S., Shevchenko, V.P., Kirpotin, S.N., Kulizhsky, S.P., Kolesnichenko, L.G., Zemtzov, V.A., Sinkinov, V.V., Pokrovsky, O.S., 2015. Seasonal dynamics of organic carbon and metals in thermokarst lakes from the discontinuous permafrost zone of western Siberia. Biogeosciences 12, 3009–3028. https://doi.org/10.5194/bg-12-3009-2015

Mann, P.J., Davydova, A., Zimov, N., Spencer, R.G.M., Davydov, S., Bulygina, E., Zimov, S., Holmes, R.M., 2012. Controls on the composition and lability of dissolved organic matter in Siberia's Kolyma River basin. J. Geophys. Res. Biogeosciences 117. https://doi.org/10.1029/2011JG001798

Mann, P.J., Eglinton, T.I., McIntyre, C.P., Zimov, N., Davydova, A., Vonk, J.E., Holmes, R.M., Spencer, R.G.M., 2015. Utilization of ancient permafrost carbon in headwaters of Arctic fluvial networks. Nat. Commun. 6, 7856. https://doi.org/10.1038/ncomms8856

McKnight, D.M., Boyer, E.W., Westerhoff, P.K., Doran, P.T., Kulbe, T., Andersen, D.T., 2001. Spectrofluorometric characterization of dissolved organic matter for indication of precursor organic material and aromaticity. Limnol. Oceanogr. 46, 38–48. https://doi.org/10.4319/lo.2001.46.1.0038

Michaelson, G.J., Ping, C.L., Kling, G.W., Hobbie, J.E., 1998. The character and bioactivity of dissolved organic matter at thaw and in the spring runoff waters of the arctic tundra North Slope, Alaska. J. Geophys. Res. Atmospheres 103, 28939–28946. https://doi.org/10.1029/98JD02650

Neff, J.C., Finlay, J.C., Zimov, S.A., Davydov, S.P., Carrasco, J.J., Schuur, E. a. G., Davydova, A.I., 2006. Seasonal changes in the age and structure of dissolved organic carbon in Siberian rivers and streams. Geophys. Res. Lett. 33. https://doi.org/10.1029/2006GL028222

Obernosterer, I., Benner, R., 2004. Competition between biological and photochemical processes in the mineralization of dissolved organic carbon. Limnol. Oceanogr. 49, 117–124. https://doi.org/10.4319/lo.2004.49.1.0117

Olefeldt, D., Roulet, N.T., 2014. Permafrost conditions in peatlands regulate magnitude, timing, and chemical composition of catchment dissolved organic carbon export. Glob. Change Biol. 20, 3122–3136. https://doi.org/10.1111/gcb.12607

Olefeldt, D., Roulet, N.T., 2012. Effects of permafrost and hydrology on the composition and transport of dissolved organic carbon in a subarctic peatland complex. J. Geophys. Res. Biogeosciences 117. https://doi.org/10.1029/2011JG001819

Palmer, S.M., Evans, C.D., Chapman, P.J., Burden, A., Jones, T.G., Allott, T.E.H., Evans, M.G., Moody, C.S., Worrall, F., Holden, J., 2016. Sporadic hotspots for physico-chemical retention of aquatic organic carbon: from peatland headwater source to sea. Aquat. Sci. 78, 491–504. https://doi.org/10.1007/s00027-015-0448-x

Panneer Selvam, B., Lapierre, J.-F., Soares, A.R.A., Bastviken, D., Karlsson, J., Berggren, M., 2019. Photo-reactivity of dissolved organic carbon in the freshwater continuum. Aquat. Sci. 81, 57. https://doi.org/10.1007/s00027-019-0653-0

Payandi-Rolland, D., 2020. Data from the DOM biodegradation along a hydrological continuum in permafrost peatlands. https://doi.org/10.17632/K9J72KJ6JS.1

Peacock, M., Evans, C.D., Fenner, N., Freeman, C., Gough, R., Jones, T.G., Lebron, I., 2014. UV-visible absorbance spectroscopy as a proxy for peatland dissolved organic carbon (DOC) quantity and quality: considerations on wavelength and absorbance

degradation. Environ. Sci. Process. Impacts 16, 1445–1461. https://doi.org/10.1039/C4EM00108G

Petrescu, A.M.R., Van Huissteden, J.C., Jackowicz-Korczynski, M., Yurova, A., Christensen, T.R., Crill, P.M., Maximov, T.C., 2007. Modelling CH_4 emissions from arctic wetlands: effects of hydrological parameterization. Biogeosciences Discuss. 4, 3195–3227.

Peura, S., Wauthy, M., Simone, D., Eiler, A., Einarsdóttir, K., Rautio, M., Bertilsson, S., 2020. Ontogenic succession of thermokarst thaw ponds is linked to dissolved organic matter quality and microbial degradation potential. Limnol. Oceanogr. 65, S248–S263. https://doi.org/10.1002/lno.11349

Pokrovsky, O.S., Manasypov, R.M., Loiko, S.V., Shirokova, L.S., 2016. Organic and organo-mineral colloids in discontinuous permafrost zone. Geochim. Cosmochim. Acta 188, 1–20. https://doi.org/10.1016/j.gca.2016.05.035

Pokrovsky, O.S., Shirokova, L.S., Kirpotin, S.N., Audry, S., Viers, J., Dupré, B., 2011. Effect of permafrost thawing on organic carbon and trace element colloidal speciation in the thermokarst lakes of western Siberia. Biogeosciences 8, 565–583. https://doi.org/10.5194/bg-8-565-2011

Raudina, T.V., Loiko, S.V., Lim, A., Manasypov, R.M., Shirokova, L.S., Istigechev, G.I., Kuzmina, D.M., Kulizhsky, S.P., Vorobyev, S.N., Pokrovsky, O.S., 2018. Permafrost thaw and climate warming may decrease the CO2, carbon, and metal concentration in peat soil waters of the Western Siberia Lowland. Sci. Total Environ. 634, 1004–1023. https://doi.org/10.1016/j.scitotenv.2018.04.059

Rocher-Ros, G., Sponseller, R.A., Bergström, A.-K., Myrstener, M., Giesler, R., 2020. Stream metabolism controls diel patterns and evasion of CO2 in Arctic streams. Glob. Change Biol. 26, 1400–1413. https://doi.org/10.1111/gcb.14895

Roehm, C.L., Giesler, R., Karlsson, J., 2009. Bioavailability of terrestrial organic carbon to lake bacteria: The case of a degrading subarctic permafrost mire complex. J. Geophys. Res. Biogeosciences 114. https://doi.org/10.1029/2008JG000863

Serikova, S., Pokrovsky, O.S., Ala-Aho, P., Kazantsev, V., Kirpotin, S.N., Kopysov, S.G., Krickov, I.V., Laudon, H., Manasypov, R.M., Shirokova, L.S., Soulsby, C., Tetzlaff, D., Karlsson, J., 2018. High riverine CO 2 emissions at the permafrost boundary of Western Siberia. Nat. Geosci. 1. https://doi.org/10.1038/s41561-018-0218-1

Serikova, S., Pokrovsky, O.S., Laudon, H., Krickov, I.V., Lim, A.G., Manasypov, R.M., Karlsson, J., 2019. High carbon emissions from thermokarst lakes of Western Siberia. Nat. Commun. 10, 1552. https://doi.org/10.1038/s41467-019-09592-1

Shirokova, L.S., Chupakov, A.V., Zabelina, S.A., Neverova, N.V., Payandi-Rolland, D., Causserand, C., Karlsson, J., Pokrovsky, O.S., 2019. Humic surface waters of frozen peat bogs (permafrost zone) are highly resistant to bio- and photodegradation. Biogeosciences 16, 2511–2526. https://doi.org/10.5194/bg-16-2511-2019

Spencer, R.G.M., Mann, P.J., Dittmar, T., Eglinton, T.I., McIntyre, C., Holmes, R.M., Zimov, N., Stubbins, A., 2015. Detecting the signature of permafrost thaw in Arctic rivers. Geophys. Res. Lett. 42, 2830–2835. https://doi.org/10.1002/2015GL063498

Striegl, R.G., Aiken, G.R., Dornblaser, M.M., Raymond, P.A., Wickland, K.P., 2005. A decrease in discharge-normalized DOC export by the Yukon River during summer through autumn. Geophys. Res. Lett. 32. https://doi.org/10.1029/2005GL024413

Tang, J., Yurova, A.Y., Schurgers, G., Miller, P.A., Olin, S., Smith, B., Siewert, M.B., Olefeldt, D., Pilesjö, P., Poska, A., 2018. Drivers of dissolved organic carbon export in a subarctic catchment: Importance of microbial decomposition, sorption-desorption, peatland and lateral flow. Sci. Total Environ. 622–623, 260–274. https://doi.org/10.1016/j.scitotenv.2017.11.252

Valle, J., Gonsior, M., Harir, M., Enrich-Prast, A., Schmitt-Kopplin, P., Bastviken, D., Conrad, R., Hertkorn, N., 2018. Extensive processing of sediment pore water dissolved organic matter during anoxic incubation as observed by high-field mass spectrometry (FTICR-MS). Water Res. 129, 252–263. https://doi.org/10.1016/j.watres.2017.11.015

Vigneron, A., Lovejoy, C., Cruaud, P., Kalenitchenko, D., Culley, A., Vincent, W.F., 2019. Contrasting Winter Versus Summer Microbial Communities and Metabolic Functions in a Permafrost Thaw Lake. Front. Microbiol. 10. https://doi.org/10.3389/fmicb.2019.01656

Vonk, J., Tank, S., Mann, P., Spencer, R., Treat, C., Striegl, R., Abbott, B., Wickland, K., 2015. Biodegradability of dissolved organic carbon in permafrost soils and aquatic systems: a meta-analysis. Biogeosciences BG 12, 6915–6930.

Vonk, J.E., Gustafsson, Ö., 2013. Permafrost-carbon complexities. Nat. Geosci. 6, 675–676. https://doi.org/10.1038/ngeo1937

Vonk, J.E., Tank, S.E., Walvoord, M.A., 2019. Integrating hydrology and biogeochemistry across frozen landscapes. Nat. Commun. 10, 1–4. https://doi.org/10.1038/s41467-019-13361-5

Walvoord, M.A., Striegl, R.G., 2007. Increased groundwater to stream discharge from permafrost thawing in the Yukon River basin: Potential impacts on lateral export of carbon and nitrogen. Geophys. Res. Lett. 34. https://doi.org/10.1029/2007GL030216

Weishaar, J.L., Aiken, G.R., Bergamaschi, B.A., Fram, M.S., Fujii, R., Mopper, K., 2003. Evaluation of Specific Ultraviolet Absorbance as an Indicator of the Chemical Composition and Reactivity of Dissolved Organic Carbon. Environ. Sci. Technol. 37, 4702–4708. https://doi.org/10.1021/es030360x

Wickland, K.P., Aiken, G.R., Butler, K., Dornblaser, M.M., Spencer, R.G.M., Striegl, R.G., 2012. Biodegradability of dissolved organic carbon in the Yukon River and its tributaries: Seasonality and importance of inorganic nitrogen: BIODEGRADABLE DOC IN THE YUKON RIVER. Glob. Biogeochem. Cycles 26, n/a-n/a. https://doi.org/10.1029/2012GB004342

Wickland, K.P., Neff, J.C., Aiken, G.R., 2007. Dissolved Organic Carbon in Alaskan Boreal Forest: Sources, Chemical Characteristics, and Biodegradability. Ecosystems 10, 1323–1340. https://doi.org/10.1007/s10021-007-9101-4

Wik, M., Crill, P.M., Varner, R.K., Bastviken, D., 2013. Multiyear measurements of ebullitive methane flux from three subarctic lakes. J. Geophys. Res. Biogeosciences 118, 1307–1321. https://doi.org/10.1002/jgrg.20103

Figures

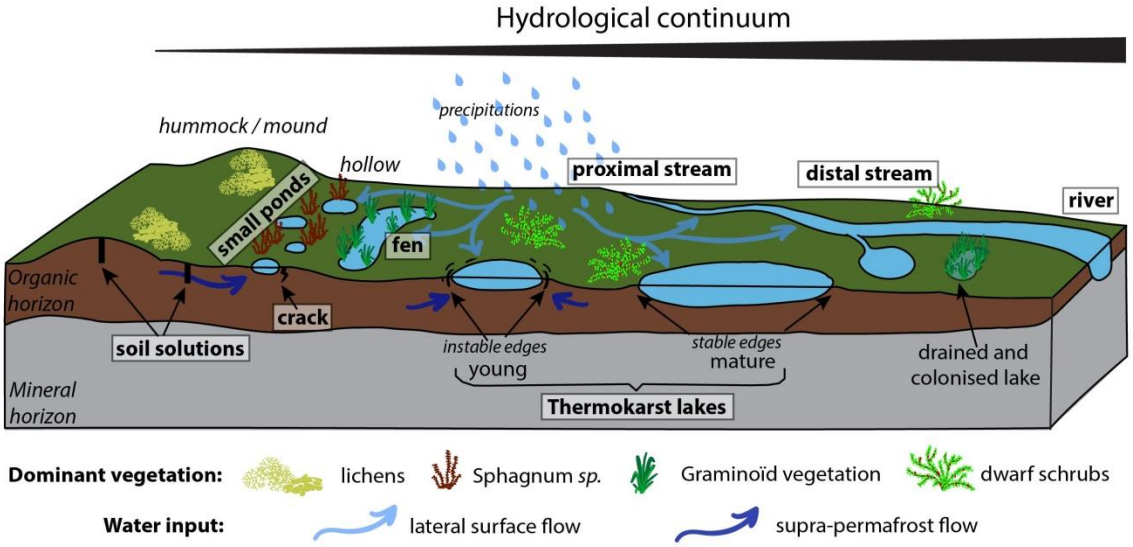

Figure 1: Schematic of a hydrological continuum in the discontinuous permafrost region. The hydrological continuum represents a progression of wetland water habitats from gravitational soil water in soil pits and cracks to small ponds, fens, lakes, streams and rivers. While the soil solutions represent the upper end of the continuum the rivers are the receiving system at the other end of the transition. Note that either the vertical or horizontal scales are not representative.

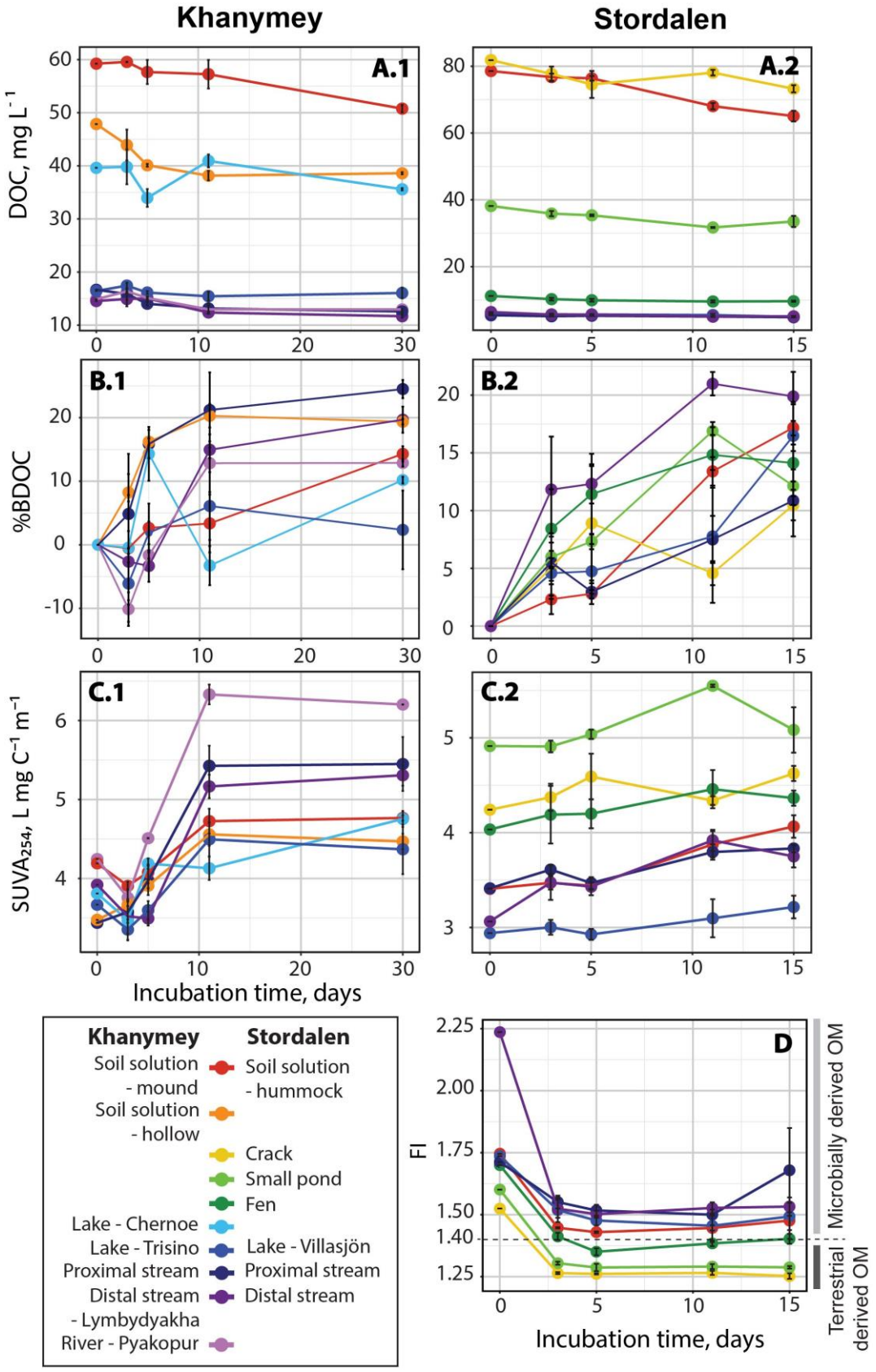

Figure 2: DOC concentration (mg L^{-1}, **A**), BDOC (%, **B**), SUVA (L mg C^{-1} m^{-1}, **C**) of the Khanymey (**.1**) and Stordalen (**.2**) hydrological continuum; and FI evolution of the Stordalen continuum during incubation time (**D**). Note that the total incubation time is 30 days for Khanymey continuum and 15 days for Stordalen continuum.

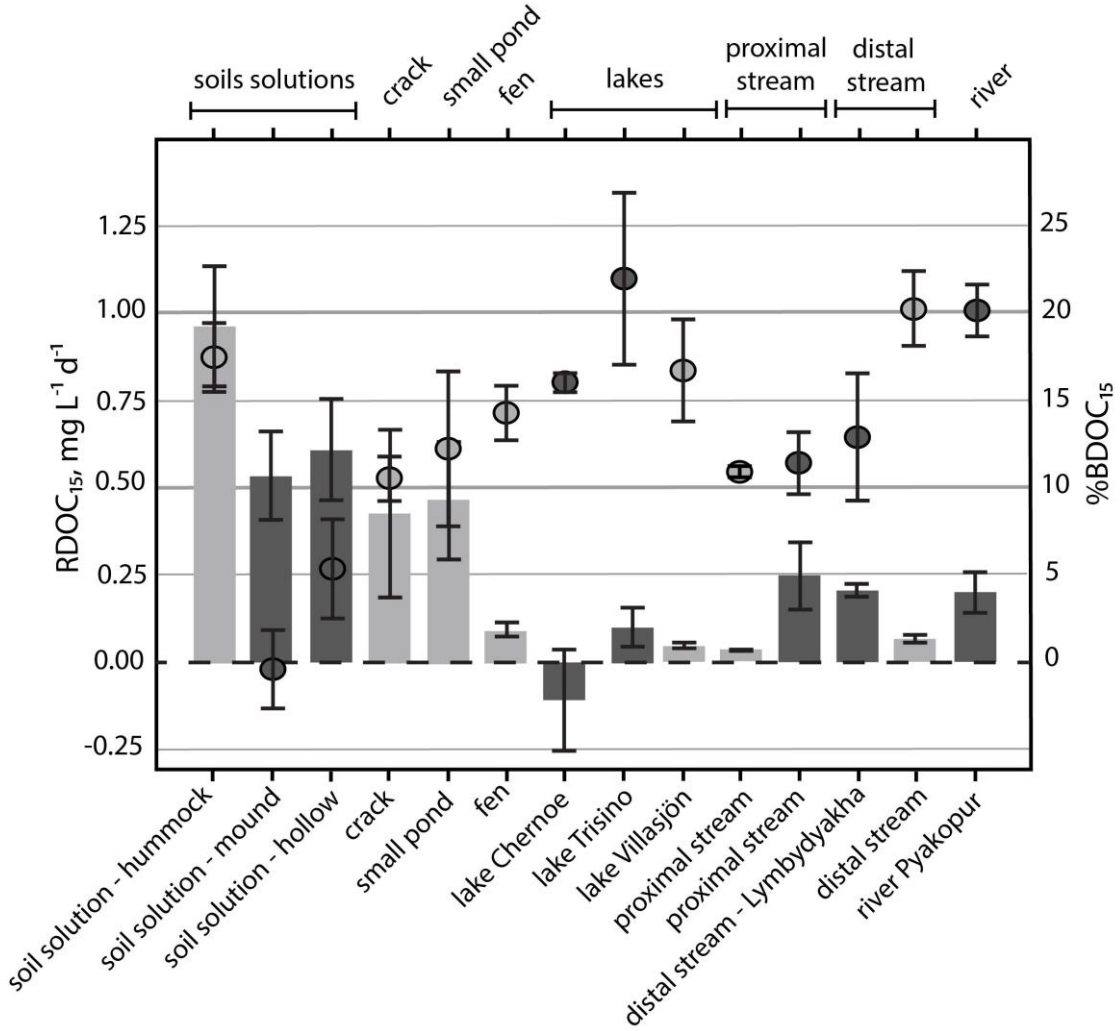

Figure 3: The removal rate of dissolved organic carbon ($RDOC_{15}$) of waters along the hydrological continuum (HC) after 15 days of incubations (bars and left y-axes). The filled circles show the biodegradable DOC ($BDOC_{15}$) after 15 days of incubations from the same HC. The waters are from 15 locations across two HC´s: one in northern Sweden (Stordalen; light grey fill for circle and bars) and one in western Siberia (Khanymey; dark gray for circle fill and bars). The sites are represented starting from the left with the upper end of the HC and the receiving systems to the right (see figure 1). The error bars denote one standard deviation.

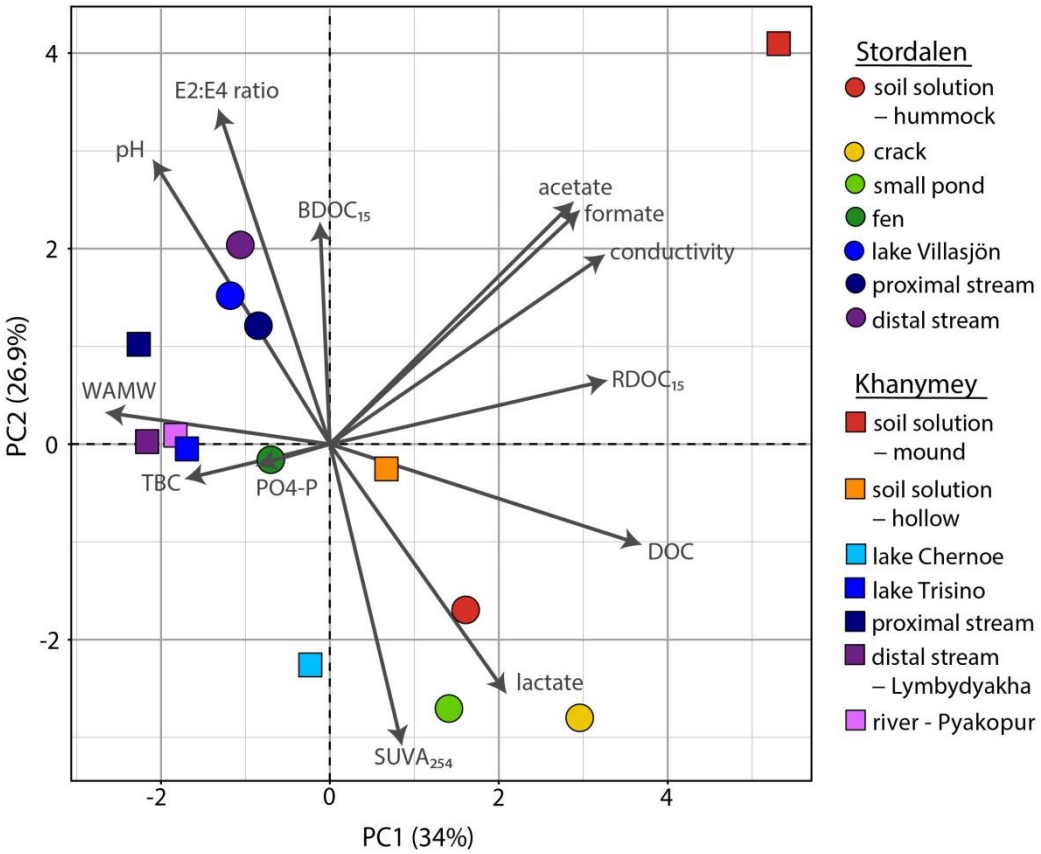

Figure 4: Biplot of the individual PCA on waters from Stordalen (circle) and Khanymey (square) hydrological continuum and variable correlation plot (black arrow).

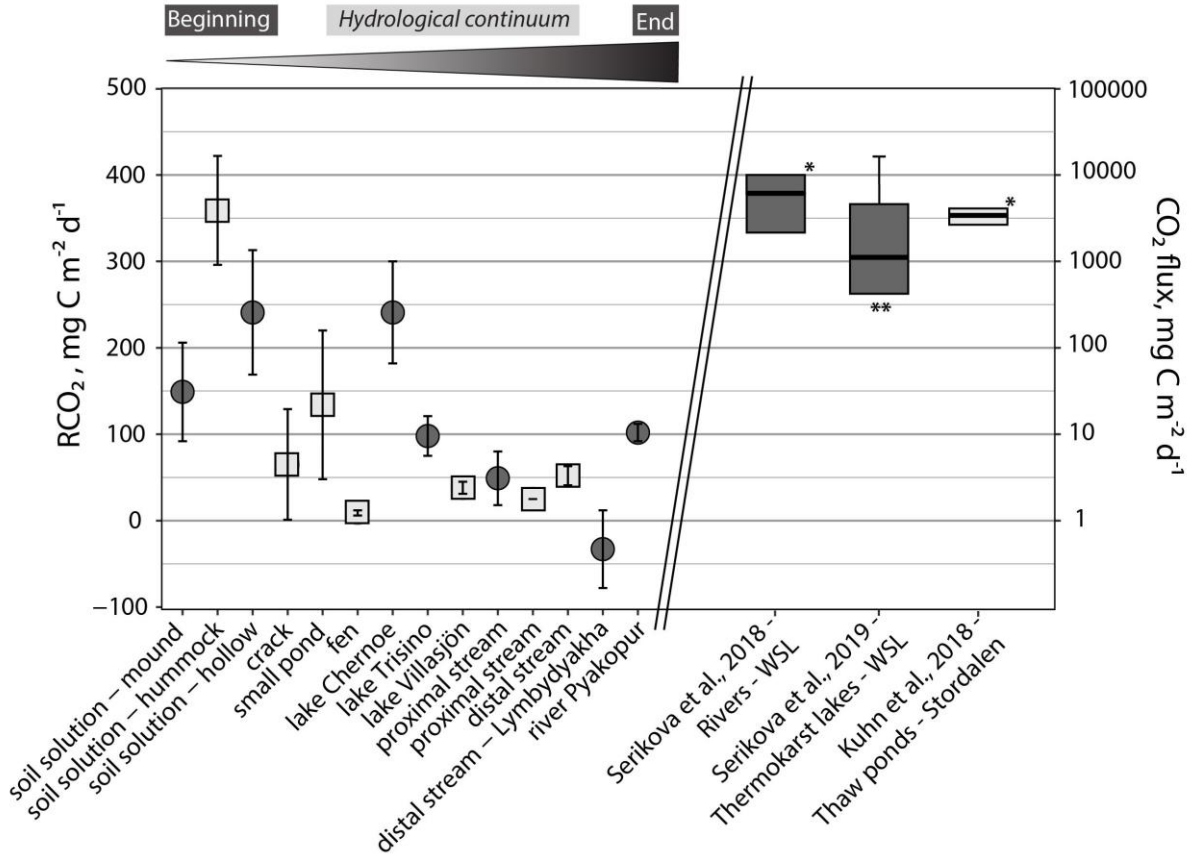

814

815 **Figure 5:** Left axis: Calculated potential CO_2 fluxes (mean ± SD) emitted by biodegradation
816 (RCO_2) of waters from the Khanymey (black circles) and Stordalen (grey squares)
817 hydrological continuum. Right axis: CO_2 emissions (mg C m^{-2} d^{-1}, log scale) field-based
818 estimated from other studies in Khanymey region (dark grey boxplot) for rivers (Serikova et
819 al., 2018) and thermokarst lakes (Serikova et al., 2019) ; and in thaw ponds from the
820 Stordalen region (light grey boxplot, Kuhn et al. (2018)). The box encloses 50% of the data
821 and the horizontal bar marks the median. Whiskers extend to the outermost data-points. ***** No
822 outermost data-points are given for those studies. ****** Negative values for the minimum
823 outermost data-point